# The Switching Fractional Order Chaotic System and Its Application to Image Encryption

Jialin Hou, Rui Xi, Ping Liu, and Tianliang Liu

***Abstract*—Many studies on fractional order chaotic systems and secure communications have been carried out, however, switching fractional order chaotic system and its application to image encryption have not been explored yet. In this paper, a new switching fractional order chaotic system is proposed, containing fractional order Chen system and the other two fractional order chaotic systems. Chaotic attractors and dynamical analysis including Lyapunov exponent, bifurcation diagram, fractal dimension, dissipation, stability and symmetry are shown firstly. After that, some circuit simulations through Multisim are presented. By controlling switch $k_1$ and $k_2$, switching among the three fractional order chaotic subsystems can be realized. Finally, we apply the switching fractional order chaotic system to image encryption using exclusive or (XOR) encryption algorithm. The encryption scheme could increase randomness and improve speed of encryption.**

***Index Terms*—Fractional order chaotic system, image encryption, subsystem, switching.**

## I. Introduction

With the rapid development of computer and network technology, the problem of security in image information transmission and storage draws more attention [1], and image encryption has become a hot topic in public. Image encryption is far different from text encryption and more complicated owing to some internal features [2]. Chaotic properties such as boundedness, intrinsic randomness and sensitivity to initial conditions meet the demand for image encryption. In the past years, theory and control of integer order chaotic systems have been explored such as Lorenz system [3], [4], Chua's system [5], Chen system [6], [7], Liu system [8]−[10] and Lu system [11]−[13]. Studies on fractional order chaotic systems including fractional order Chen system [14]−[16], fractional order Lorenz system [17], fractional order Liu system [18] and fractional order Chua's system [19] have also attracted many researchers. In terms of secure communication, lower dimensional integer chaotic systems are more easily-implemented than higher ones, whereas security of higher dimensional integer chaotic systems is better than lower ones [17]. Compared with integer order chaotic system, fractional order chaotic system has more complex chaotic characteristics and more complicated topological structures. When applied to image encryption, the fractional order system could support a larger key space, enhance security and withstand the attacks effectively. At present, articles could be found about fractional order chaotic systems applied to secure communications in [20]−[22].

Fractional calculus has a long history of more than 300 years, we know the Riemann-Liouvile definition of fractional order integral [23] is

$$\frac{d^{\alpha}f(t)}{dt^{\alpha}}=\frac{1}{\Gamma(m-a)}\frac{d^{m}}{dt^{m}}\int_{t_0}^{t}\frac{f(\tau)}{(t-\tau)^{\alpha-m+1}}d\tau$$

where $m-1<\alpha<m$, $m\in\mathbb{N}$.

When all the initial conditions are zero, the Laplace transform of the Riemann-Liouville definition is

$$L\left\{\frac{d^{q}f(t)}{dt^{q}}\right\}=s^{q}L\{f(t)\}.$$

The rest of the paper is organized as follows. Section II gives dynamical analyses of the proposed switching fractional order chaotic system. Section III presents circuit simulations. In Section IV, application of the switching fractional order chaotic system to image encryption is introduced and some conclusions are given in the last.

## II. System Composition and Dynamical Properties

### A. System Composition

The fractional order Chen system is:

$$\begin{cases}\frac{d^{q}x}{dt^{q}}=a(y-x)\\ \frac{d^{q}y}{dt^{q}}=(c-a)x-xz+cy\\ \frac{d^{q}z}{dt^{q}}=xy-bz\end{cases}\tag{1}$$

where $a$, $b$ and $c$ are real parameters, and $a=35$, $b=3$ and $c=28$, $q$ is called the fractional order and $q=0.9$. Keeping the values of $a$, $b$, $c$ and $q$ unchanged, we switch the subsystem

Manuscript received September 1, 2015; accepted January 4, 2016. This work was supported by National Natural Science Foundation of China (31301080), China Postdoctoral Science Foundation Project (2015M582122, 2016T90644), National Key Technology Support Program of China (2015BAF13B00), Natural Science Foundation of Shandong Province (ZR2015FL001), and the Open Project of State Key Laboratory of Crop Biology (2013KF10). Recommended by Associate Editor Dingyü Xue.

Citation: J. L. Hou, R. Xi, P. Liu, and T. L. Liu, "The switching fractional order chaotic system and its application to image encryption," *IEEE/CAA Journal of Automatica Sinica*, vol. 4, no. 2, pp. 381−388, Apr. 2017.

J. L. Hou and R. Xi are with Shandong Key Laboratory of Gardening Machinery and Equipment, College of Mechanical and Electrical Engineering, Agricultural University of Shandong, Tai'an 271018, China (e-mail: jlhou@sdau.edu.cn; 18854887517@163.com).

P. Liu is with Shandong Key Laboratory of Gardening Machinery and Equipment, College of Mechanical and Electrical Engineering, Agricultural University of Shandong, Tai'an 271018, China, and the School of Computer Science and Technology, Dalian University of Technology, Dalian 116023, China (e-mail: liupingshd@126.com).

T. L. Liu is with Shandong Key Laboratory of Gardening Machinery and Equipment, College of Mechanical and Electrical Engineering, Agricultural University of Shandong, Tai'an 271018, China, and the Department of Mechanical and Electronic Engineering, Taishan Vocational and Technical College, Tai'an 271018, China (e-mail: 30599345@qq.com).

Color version of one or more of the figures in this paper are available online at http://ieeexplore.ieee.org.

Digital Object Identifier 10.1109/JAS.2016.7510127

(1) by replacing $xy$ with $x^2$ in the nonlinear term and then obtain the subsystem (2):

$$\begin{cases} \frac{d^q x}{dt^q} = a(y-x) \\ \frac{d^q y}{dt^q} = (c-a)x - xz + cy \\ \frac{d^q z}{dt^q} = x^2 - bz. \end{cases} \tag{2}$$

Next, by the substitution of $y^2$ for $x^2$ in the nonlinear term of the subsystem (2), the subsystem (3) could be obtained:

$$\begin{cases} \frac{d^q x}{dt^q} = a(y-x) \\ \frac{d^q y}{dt^q} = (c-a)x - xz + cy \\ \frac{d^q z}{dt^q} = y^2 - bz. \end{cases} \tag{3}$$

### B. Dynamical Properties of System

The subsystem (1) has following basic dynamical properties:

*1) Lyapunov Exponents and Bifurcation Diagram:* According to the definition of Lyapunov exponents, when selecting parameters $a = 35$, $b = 3$, $c = 28$ with initial values $x(0) = 3$, $y(0) = 1$, and $z(0) = 5$, we could get the Lyapunov exponents of subsystem (1) as: $L_1 = 2.0074$, $L_2 = 0$ and $L_3 = -19.2303$. The subsystem (1) displays chaotic behavior since one of the Lyapunov exponents is positive [24]. For the case of choosing the same parameters and initial conditions, chaotic attractors of the subsystem (1) in different phase planes are shown in Fig. 1.

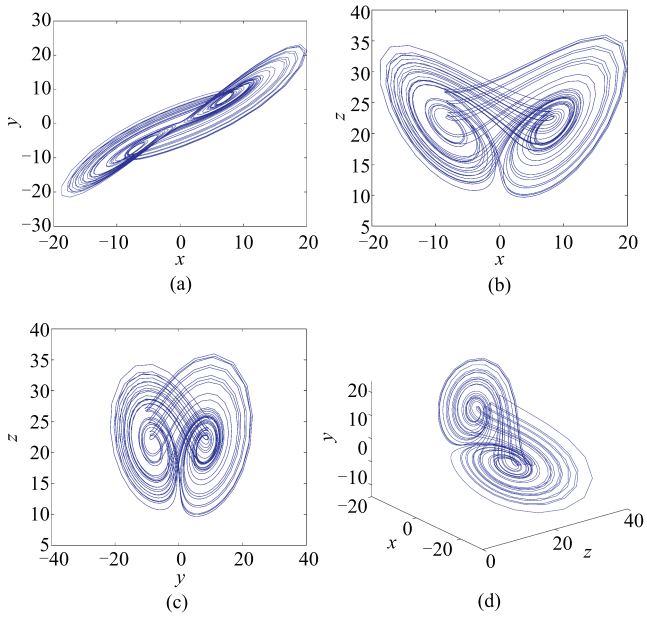


Fig. 1. Chaotic attractors of the subsystem (1) in different phase planes.

Bifurcation means a change, a splitting apart and a division into two branches. The bifurcation diagram and Lyapunov exponent spectrum for subsystem (1) due to the variation of parameters $a$ and $b$ are investigated in this paper. For subsystem (2) and subsystem (3), those could also be discussed similarly and will be omitted.

From Fig. 2, we could see that when $33 < a < 46$, subsystem (1) is chaotic.

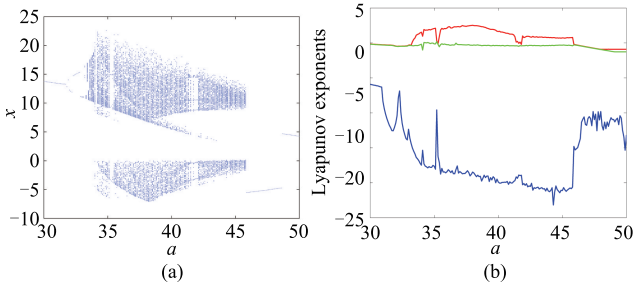


Fig. 2. Bifurcation diagram and Lyapunov exponent spectrum with respect to parameter $a$. (a) Bifurcation diagram. (b) Lyapunov exponent spectrum.

From Fig. 3, conclusion could be obtained that when $0 < b < 4.2$, subsystem (1) shows chaotic behavior.

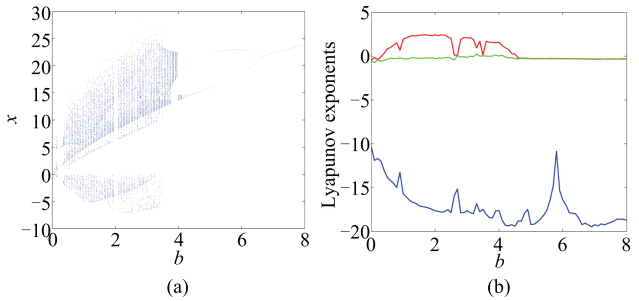


Fig. 3. Bifurcation diagram and Lyapunov exponent spectrum with respect to parameter $b$. (a) Bifurcation diagram. (b) Lyapunov exponent spectrum.

*2) Fractal Dimension:* For this case, the formula is

$$D = j + \frac{1}{|L_{j+1}|}\sum_{i=1}^{j} L_j = 2 + \frac{L_1 + L_2}{|L_3|} = 2.1044 \tag{4}$$

therefore, the Lyapunov dimension of subsystem (1) is fractal dimension.

*3) Dissipation:* The formula is

$$\nabla V = \frac{\partial \dot{x}}{\partial x} + \frac{\partial \dot{y}}{\partial y} + \frac{\partial \dot{z}}{\partial z} = -a + c - b = -10 < 0 \tag{5}$$

so the subsystem (1) is dissipative, converging at exponential rate $e^{-10t}$. In other words, the initial volume element is $V(0)$ and becomes $V(t) = V(0)e^{-10t}$ in time $t$. When $t \to \infty$, every volume element which contains trajectories of the subsystem (1) shrinks to zero with the rate of exponential convergence.

*4) Equilibrium Points and Stability:* The equilibrium points of subsystem (1) could be calculated by making subsystem (1) $= 0$, we get three equilibrium points of the subsystem (1) as

$$E_1 = (0,\ 0,\ 0)$$

$$E_2 = (7.937,\ 7.937,\ 21)$$

$$E_3 = (-7.937,\ -7.937,\ 21).$$

By linearizing the subsystem (1) at point $E_1$, the Jacobian matrix $J_0$ could be obtained:

$$J_0 = \begin{pmatrix} -35 & 35 & 0 \\ -7 & 28 & 0 \\ 0 & 0 & -3 \end{pmatrix}. \tag{6}$$

TABLE I
DYNAMICAL PROPERTIES OF THE SUBSYSTEM (2) AND SUBSYSTEM (3)

| Dynamical properties | The subsystem (2) | The subsystem (3) |
|---|---|---|
| Lyapunov exponents | $LE_1 = 2.0017,\ LE_2 = 0,\ LE_3 = -19.2001$ | $LE_1 = 2.0019,\ LE_2 = 0,\ LE_3 = -19.2011$ |
| Fractal dimension | $D = 2 + \frac{L_1+L_2}{\lvert L_3\rvert} = 2.1043$ | $D = 2 + \frac{L_1+L_2}{\lvert L_3\rvert} = 2.1042$ |
| Dissipation | $\frac{\partial \dot{x}}{\partial x} + \frac{\partial \dot{y}}{\partial y} + \frac{\partial \dot{z}}{\partial z} = -10 < 0$ | $\frac{\partial \dot{x}}{\partial x} + \frac{\partial \dot{y}}{\partial y} + \frac{\partial \dot{z}}{\partial z} = -10 < 0$ |
| Equilibrium points | $E_1 = (0,\ 0,\ 0),\ E_2 = (7.937,\ 7.937,\ 21)$ $E_3 = (-7.937,\ -7.937,\ 21)$ | $E_1 = (0,\ 0,\ 0),\ E_2 = (7.937,\ 7.937,\ 21)$ $E_3 = (-7.937,\ -7.937,\ 21)$ |
| Symmetry | Symmetrical about the $z$-axis | Symmetrical about the $z$-axis |

The characteristic polynomial of Jacobian matrix $J_0$ is

$$(-35-\lambda)(28-\lambda)(-3-\lambda)+7\times 35(-3-\lambda)=0. \quad (7)$$

From (7), we could obtain eigenvalues of the linearized subsystem (1) at point $E_1$: $\lambda_1 = -30.8359$, $\lambda_2 = 23.8359$, $\lambda_3 = -3$. According to [25], we learn that when and only when the real parts of all eigenvalues of system at equilibrium points are negative, system is stable. As a result, the subsystem (1) is unstable at the equilibrium point $E_1$.

In the same way, eigenvalues of the corresponding linearized subsystem (1) at point $E_2$ and $E_3$ could also be obtained:

$$\begin{aligned} E_2 : \lambda_1 &= -18.4280 \\ \lambda_2 &= 4.2140 + 14.8846i \\ \lambda_3 &= 4.2140 - 14.8846i \end{aligned}$$

$$\begin{aligned} E_3 : \lambda_1 &= -18.4280 \\ \lambda_2 &= 4.2140 + 14.8846i \\ \lambda_3 &= 4.2140 - 14.8846i. \end{aligned}$$

Eigenvalues at $E_2$ and $E_3$ are complex conjugate roots with positive real part, so, the subsystem (1) is unstable at equilibrium points $E_2$ and $E_3$ similarly.

*5) Symmetry:* The subsystem (1) is symmetrical about the $z$-axis on account of its invariance after the transformation $(x, y, z) \rightarrow (-x, -y, z)$. The dynamical properties of the subsystem (2) and subsystem (3) could also be analysed similarly. With the selection of parameters $a = 35$, $b = 3$, $c = 28$ and initial values $\dot{x}(0) = 2$, $\dot{y}(0) = 4$, $\dot{z}(0) = 4$, chaotic attractors of the subsystem (2) in different phase planes are plotted in Fig. 4.

When selecting parameters $a = 35$, $b = 3$, $c = 28$ and initial values $\ddot{x}(0) = 2$, $\ddot{y}(0) = 1$, $\ddot{z}(0) = 2$, chaotic attractors of the subsystem (3) in different phase planes are shown as Fig. 5. Dynamical properties of the two subsystems are displayed in Table I.

## III. ANALOG CIRCUIT IMPLEMENTATION

### A. Fractional Tree Circuit Unit

With respect to circuit design of fractional order chaotic system, the key point is how to design the circuit of $1/s^{0.9}$.

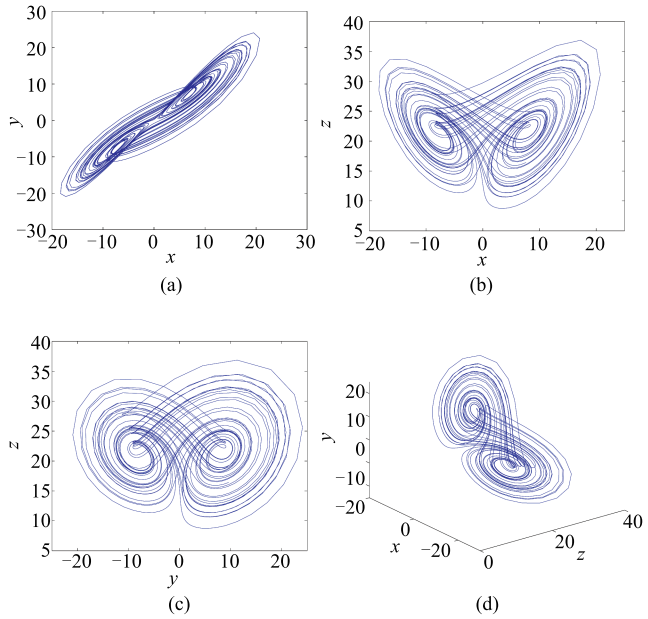


Fig. 4. Chaotic attractors of the subsystem (2) in different phase planes.

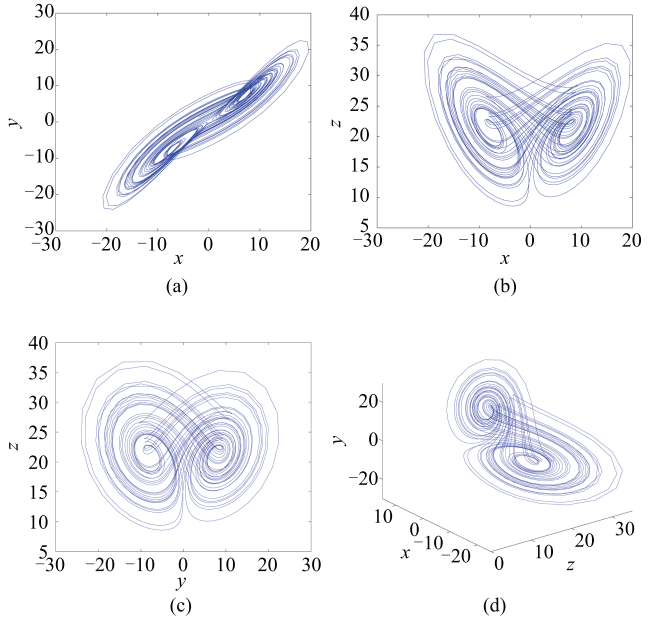


Fig. 5. Chaotic attractors of the subsystem (3) in different phase planes.

Reference [26] gave the approximate expression (8) (approximation error 2 dB) and tree circuit unit of $1/s^{0.9}$ is shown as Fig. 6.

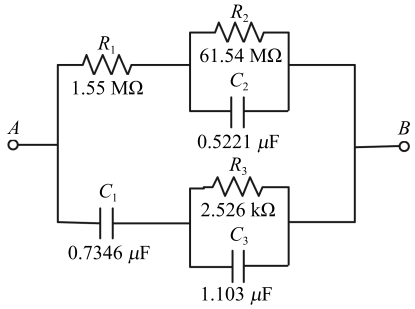


Fig. 6. Tree circuit unit.

$$\frac{1}{s^{0.9}} \approx \frac{2.2675(s+1.292)(s+215.4)}{(s+0.01292)(s+2.154)(s+359.4)}. \tag{8}$$

The transfer function of the tree circuit unit is (9), shown at the bottom of this page.

In (9), $C_0$ is a unit parameter, and let $C_0 = 1\,\mu$F, $F(s) = H(s)\cdot C_0 = 1/s^{0.9}$. Compared with (8), the values of resistances and capacitances could be calculated as follows: $R_1 = 1.55\,\text{M}\Omega$, $R_2 = 61.54\,\text{M}\Omega$, $R_3 = 2.526\,\text{k}\Omega$, $C_1 = 0.7346\,\mu$F, $C_2 = 0.5221\,\mu$F, $C_3 = 1.103\,\mu$F.

### B. Circuit Simulations

As is shown in Fig. 7, this circuit is composed of resistors, capacitors with different values, operational amplifiers LM741, analog multipliers AD633 (output gain is 0.1), analog switches and 0.9 order circuits.

When switch $k1$ connects to $x$ while $k2$ connects to $y$, or $k1$ connects to $y$ while $k2$ connects to $x$, the subsystem (1) will be obtained. Simulation results are shown in Fig. 8.

According to circuit schematic diagram, the fractional order circuit equation could be gotten:

$$\begin{cases} \frac{d^{0.9}x}{dt^{0.9}} = \frac{R_{12}}{R_{14}R_{11}C}y - \frac{R_{12}}{R_{13}R_{11}C}x \\ \frac{d^{0.9}y}{dt^{0.9}} = \frac{R_{17}}{R_{18}R_{11}C}(-x) - \frac{R_{17}}{10R_{20}R_{11}C}xz + \frac{R_{17}}{R_{21}R_{11}C}y \\ \frac{d^{0.9}z}{dt^{0.9}} = \frac{R_{23}}{10R_{24}R_{11}C}xy - \frac{R_{23}}{R_{25}R_{11}C}z. \end{cases} \tag{10}$$

When switch $k1$ connects to $x$, and $k2$ connects to $x$, the subsystem (2) will work. Simulation results are shown in Fig. 9.

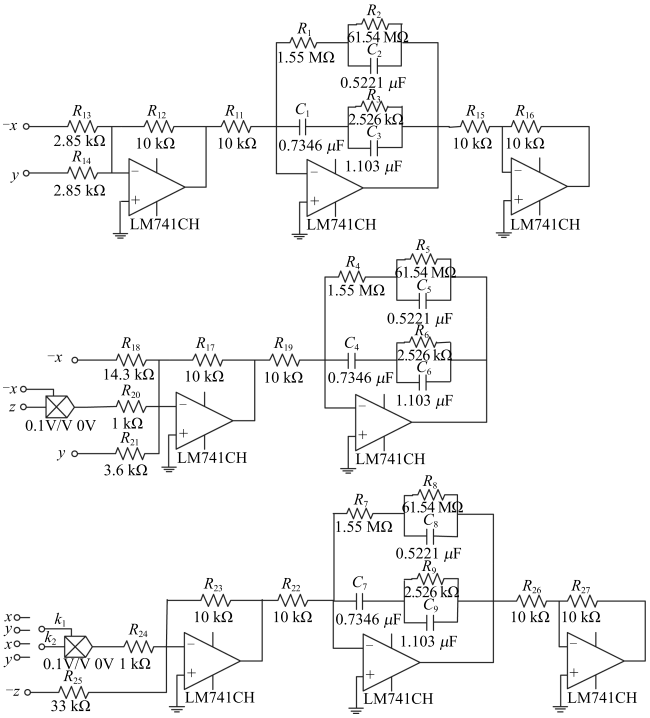


Fig. 7. Circuit schematic diagram.

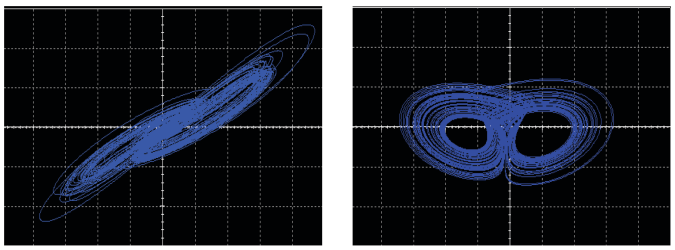

(a) (b)

Fig. 8. Circuit simulations of the subsystem (1).

In this case, the fractional order circuit equation could be written as

$$\begin{cases} \frac{d^{0.9}x}{dt^{0.9}} = \frac{R_{12}}{R_{14}R_{19}C}y - \frac{R_{12}}{R_{13}R_{19}C}x \\ \frac{d^{0.9}y}{dt^{0.9}} = \frac{R_{17}}{R_{18}R_{19}C}(-x) - \frac{R_{17}}{10R_{20}R_{19}C}xz + \frac{R_{17}}{R_{21}R_{19}C}y \\ \frac{d^{0.9}z}{dt^{0.9}} = \frac{R_{23}}{10R_{24}R_{19}C}x^2 - \frac{R_{23}}{R_{25}R_{19}C}z. \end{cases} \tag{11}$$

$$H(s) = \left[R_1 + (R_2 // \frac{1}{sC_2})\right] // \left[\frac{1}{sC_1} + (R_3 // \frac{1}{sC_3})\right]$$

$$= \frac{\frac{1}{C_0}\left[(\frac{C_0}{C_1} + \frac{C_0}{C_3})(s + \frac{R_1+R_2}{R_1C_2R_2})(s + \frac{1}{C_1R_3 + C_3R_3})\right]}{s^3 + (\frac{R_1+R_2}{R_1C_2R_2} + \frac{1}{C_3R_3} + \frac{C_1+C_3}{C_1R_1C_3})s^2 + (\frac{R_1+R_2}{R_1C_2R_2C_3R_3} + \frac{1}{R_1C_1R_3C_3} + \frac{C_1+C_3}{R_1C_1R_2C_2C_3})s + \frac{1}{R_1C_1R_2C_2R_3C_3}}. \tag{9}$$

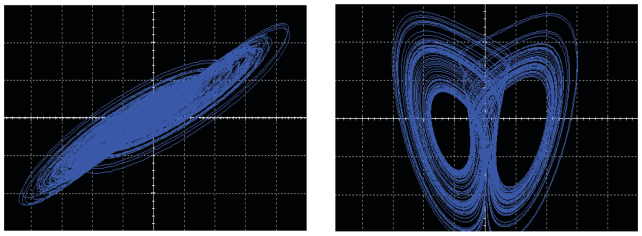

(a) (b)

Fig. 9. Circuit simulations of the subsystem (2).

When switch $k1$ is connected to $y$ while $k2$ is connected to $y$, the subsystem (3) will be in operation. Simulation results are shown in Fig. 10. Similarly, the fractional order circuit equation is given by

$$\begin{cases} \frac{d^{0.9}x}{dt^{0.9}} = \frac{R_{12}}{R_{14}R_{22}C}y - \frac{R_{12}}{R_{13}R_{22}C}x \\ \frac{d^{0.9}y}{dt^{0.9}} = \frac{R_{17}}{R_{18}R_{22}C}(-x) - \frac{R_{17}}{10R_{20}R_{22}C}xz + \frac{R_{17}}{R_{21}R_{22}C}y \\ \frac{d^{0.9}z}{dt^{0.9}} = \frac{R_{23}}{10R_{24}R_{22}C}y^2 - \frac{R_{23}}{R_{25}R_{22}C}z. \end{cases} \tag{12}$$

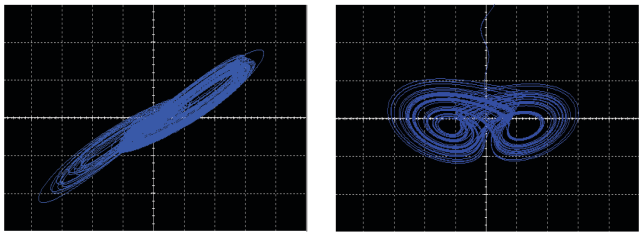

(a) (b)

Fig. 10. Circuit simulations of the subsystem (3).

Comparing (10)−(12) with (1)−(3) respectively, we could get the values of resistors in Fig. 7.

We could see that the results of circuit simulations with Multisim and numerical simulations through MATLAB are basically the same.

## IV. Application to Image Encryption

After the presentation of dynamical analyses, numerical and circuit simulations, validity of the proposed switching fractional order chaotic system is confirmed. Now, we apply it to image encryption.

### A. Description of Encryption Algorithm

In this paper, XOR operation is used in the image encryption and it has the following rule:

$$m \text{ XOR } f(z) \text{ XOR } f(z) = m \tag{13}$$

where, $m$ is pixel value of the image shown in Fig. 11 (a), $f(z)$ is key sequence generated by the switching fractional order chaotic system and $f(z)$ has the following rules:

$$f(z) = \begin{cases} z_1, & 0 \le m < 85 \\ z_2, & 85 \le m < 170 \\ z_3, & 170 \le m \le 255 \end{cases} \tag{14}$$

where $z_1$, $z_2$ and $z_3$ sequences are from the three subsystems respectively, when $0 \le m < 85$, $z_1$ is used in the image encryption, when $85 \le m < 170$, $z_2$ is used to encrypt the image and in the same way, when $170 \le m \le 255$, $z_3$ is used in the image encryption.

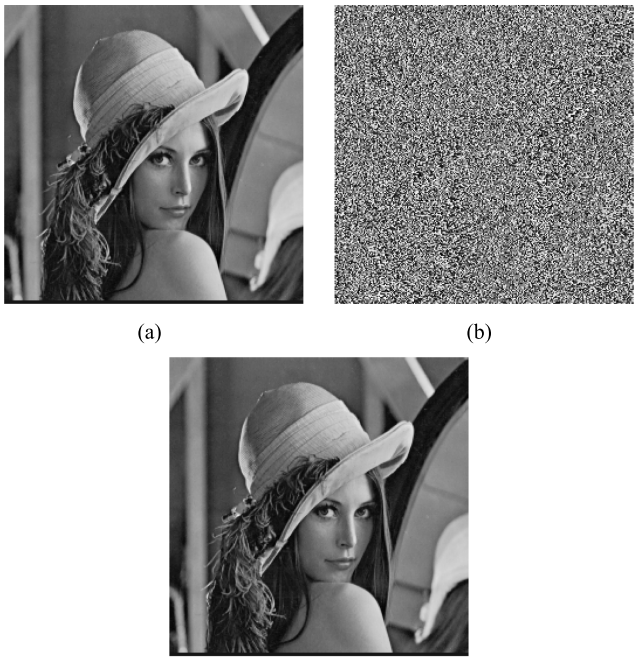

(a) (b)

(c)

Fig. 11. Process of encryption and decryption. (a) Original image. (b) Encrypted image. (c) Decrypted image.

### B. Encryption and Decryption Process

We could get the encrypted image by performing logic XOR operation between $m$ and $f(z)$, shown in Fig. 11 (b). Similarly, decrypted image could be obtained by performing the same operation between encrypted image and $f(z)$, shown in Fig. 11 (c). Therefore, process of encryption and decryption could be realized by using the same secret-key sequence. The schematic block diagram of encryption and decryption is shown in Fig. 12.

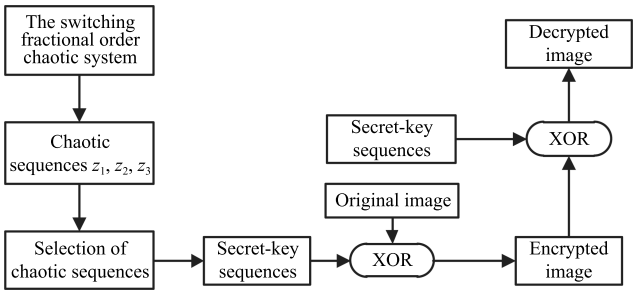


Fig. 12. The schematic block diagram of encryption and decryption.

### C. Security Analyses

*1) Histogram Analysis:* Histogram reflects the basic statistical characteristics of images. From Fig. 13, we could see a great difference between histogram of original and encrypted

image. Information of original image is well covered, which could be hardly decoded from histogram of encrypted image.

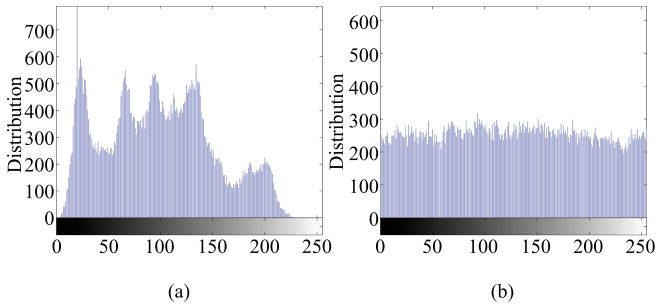


Fig. 13. Histogram. (a) Histogram of original image. (b) Histogram of encrypted image.

*2) Key Space Analysis:* In the encryption scheme, key space should be sufficiently large to resist brute-force attack. The size of key space is the total number of different keys which are used in the encryption [27]. The encryption scheme contains thirteen key parameters, which are $x(0)$, $y(0)$, $z(0)$, $\dot{x}(0)$, $\dot{y}(0)$, $\dot{z}(0)$, $\ddot{x}(0)$, $\ddot{y}(0)$, $\ddot{z}(0)$ and $a$, $b$, $c$, $q$. If the precision is $10^{-14}$, it is obvious that the total key space is $10^{14}\times10^{14}\times10^{14}\times10^{14}\times10^{14}\times10^{14}\times10^{14}\times10^{14}\times10^{14}\times10^{14}\times10^{14}\times10^{14}\times10^{14}=10^{182}$ in our encryption algorithm. Obviously, it is much larger than one in [21].

*3) Key Sensitivity Analysis:* A good encryption algorithm not only has a large key space but also is sensitive to encrypting parameters to resist attacks [22]. In the process of decrypting, we alter the key parameters slightly, when $x(0)=3+10^{-8}$ is selected in the key sequences to decrypt the image, the result is shown in Fig. 14, we could see that the proposed encryption algorithm is so sensitive to key parameters that a little variance will lead to a quite different result. The sensitivity of the other parameters are similar to $x(0)$.

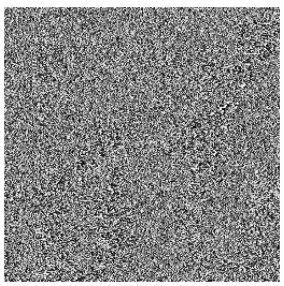

Fig. 14. Wrong decryption.

*4) Encryption Speed:* In this paper, MATLAB 7.10 is used to run the program that realizes the proposed algorithm in a personal computer with a Pentium 4 CPU 3.0 GHz, 4.0 GB RAM, 500 GB hard disk and Microsoft Windows 7 operating system. The proposed algorithm is compared with encryption algorithms in [28] and [29], comparison results between different algorithms are shown in Table II. We could see that the encryption speed of our algorithm is much faster.

### D. Color Image Encryption

*1) Procedure of Encryption and Decryption:* RGB components from the color image are extracted, as shown in Figs. 15 (a)−(d), and then XOR operation on each channel of the image using the key sequences is performed, as shown in Fig. 16.

TABLE II
COMPARISON OF ENCRYPTION SPEED BETWEEN DIFFERENT ALGORITHMS

| Algorithms | Encryption speed (MB/s) |
|---|---|
| Algorithm of [28] | 4.80 |
| Algorithm of [29] | 6.21 |
| The proposed algorithm | 8.32 |

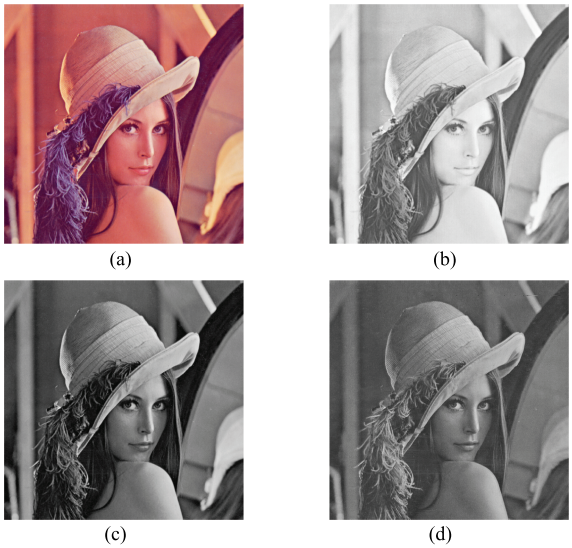


Fig. 15. Color plain-image and its R, G, B components. (a) Color plain-image. (b) R component of plain-image. (c) G component of plain-image. (d) B component of plain-image.

The decryption process is similar to that of the encryption but in the reversed order.

*2) Histogram Analysis:* The histograms of plain image and encrypted image in each channel are shown in Fig. 17. The histogram of plain image in R, G and B channel is displayed in Figs. 17 (a)−(c). Figs. 17 (d)−(f) represent the results after encryption. Obviously, no useful information can be extracted from encrypted image and we can therefore guarantee the security of image encryption. With respect to quantitative analyses, we employ variances of histograms to evaluate uniformity of distribution. The formula of histogram variance [30] is

$$\mathrm{var}(z)=\frac{1}{n^2}\sum_{i=1}^{n}\sum_{j=1}^{n}\frac{1}{2}(z_i-z_j)^2$$

the detailed calculation procedure could be referred to [30] and will not be presented here.

So, the proposed encryption algorithm could also be applied in color image. Discussions on key space and sensitivity are similar to grey-level image encryption and will be omitted.

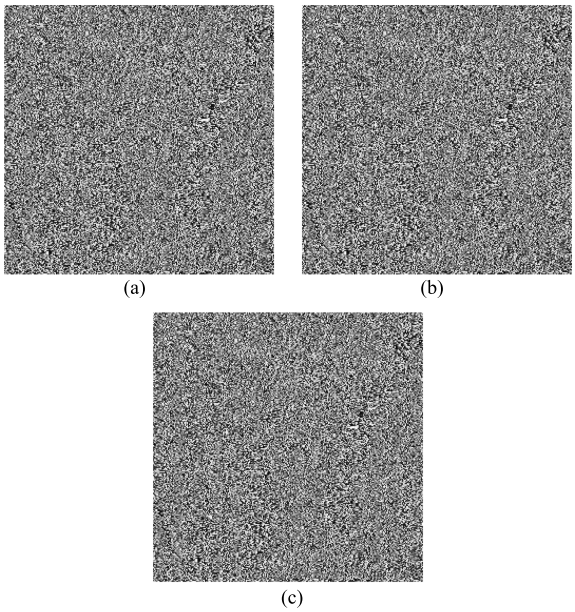


Fig. 16. The encrypted R, G, B components. (a) The encrypted R component. (b) The encrypted G component. (c) The encrypted B component.

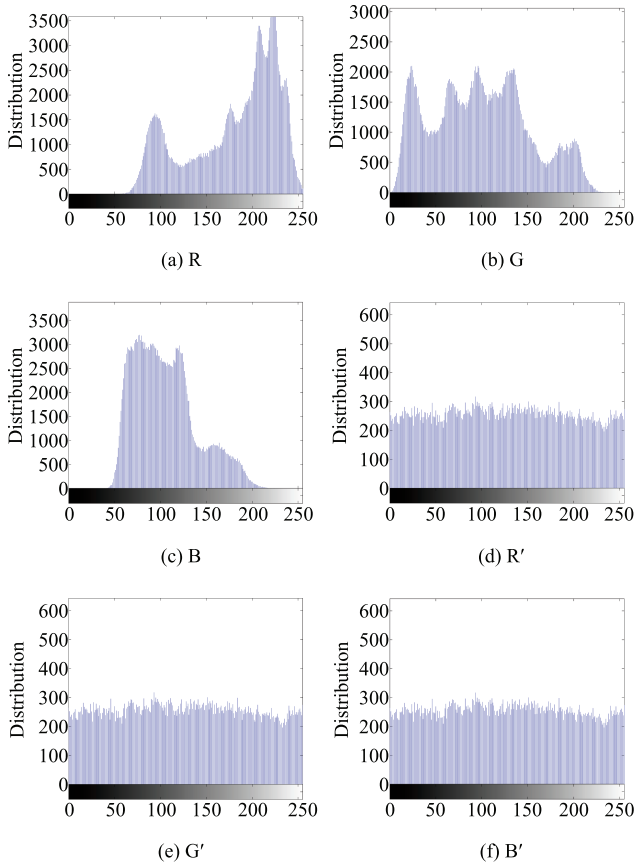


Fig. 17. Histograms of plain image and encrypted image in each channel.

## V. Conclusions

In this paper, we have studied a new switching fractional order chaotic system, which is composed of three fractional order chaotic subsystems. With regard to the switching fractional order chaotic system, chaotic attractors are shown firstly, and then dynamical properties are discussed, switching among the three subsystems is allowed by controlling switch $k1$ and $k2$, the results of circuit simulations and numerical simulations are basically the same. Therefore, the proposed switching fractional order chaotic system is valid. At last, we apply it to image encryption by using XOR operation. The security analyses show that the encryption scheme has a larger key space and higher sensitivity to key parameters. Additionally, it also has stronger randomness and faster speed in encryption process. Although the proposed system has been applied to image encryption, but it is not just limited to it. It has perfect prospects in key agreement protocol [31] and neural network [32], [33].

## References

[1] L. Y. Wang, H. J. Song, and P. Liu, "A novel hybrid color image encryption algorithm using two complex chaotic systems," *Opt. Lasers Eng.*, vol. 77, pp. 118−125, Feb. 2016.

[2] X. Y. Wang, L. Teng, and X. Qin, "A novel colour image encryption algorithm based on chaos," *Signal Process.*, vol. 92, no. 4, pp. 1101−1108, Apr. 2012.

[3] X. Y. Wang and M. J. Wang, "A hyperchaos generated from Lorenz system," *Phys. A: Statist. Mech. Appl.*, vol. 387, no. 14, pp. 3751−3758, Jun. 2008.

[4] Y. G. Zhang, J. Y. Yang, K. C. Wang, Z. P. Wang, and Y. D. Wang, "Improved wind prediction based on the Lorenz system," *Renew. Energy*, vol. 81, pp. 219−226, Sep. 2015.

[5] X. X. Liao, H. G. Luo, G. Zhang, J. G. Jian, X. J. Zong, and B. J. Xu, "New results on global synchronization of Chua's circuit," *Acta Automat. Sin.*, vol. 31, no. 2, pp. 320−326, Mar. 2005.

[6] H. P. Hu, L. F. Liu, and N. D. Ding, "Pseudorandom sequence generator based on the Chen chaotic system," *Comp. Phys. Commun.*, vol. 184, no. 3, pp. 765−768, Mar. 2013.

[7] N. Smaoui, A. Karouma, and M. Zribi, "Secure communications based on the synchronization of the hyperchaotic Chen and the unified chaotic systems," *Commun. Nonlinear Sci. Numer. Simul.*, vol. 16, no. 8, pp. 3279−3293, Aug. 2011.

[8] Y. J. Liu and G. P. Pang, "The basin of attraction of the Liu system," *Commun. Nonlinear Sci. Numer. Simul.*, vol. 16, no. 4, pp. 2065−2071, Apr. 2011.

[9] Y. K. Li, "The stability of hybrid Liu chaotic system with a sort of oscillating parameters under impulsive control," *Phys. Proc.*, vol. 24, pp. 490−495, Dec. 2012.

[10] A. E. Matouk, "Dynamical analysis, feedback control and synchronization of Liu dynamical system," *Nonlin. Anal.: Theory Meth. Appl.*, vol. 69, no. 10, pp. 3213−3224, Nov. 2008.

[11] A. Algaba, F. Fernández-Sánchez, M. Merino, and A. J. Rodríguez-Luis, "Centers on center manifolds in the Lorenz, Chen and Lü systems," *Commun. Nonlinear Sci. Numer. Simul.*, vol. 19, no. 4, pp. 772−775, Apr. 2014.

[12] G. A. Leonov and N. V. Kuznetsov, "On differences and similarities in the analysis of Lorenz, Chen, and Lu systems," *Appl. Math. Comput.*, vol. 256, pp. 334−343, Apr. 2015.

[13] A. Algaba, F. Fernández-Sánchez, M. Merino, and A. J. Rodríguez-Luis, "The Lü system is a particular case of the Lorenz system," *Phys. Lett. A*, vol. 377, no. 39, pp. 2771−2776, Nov. 2013.

[14] J. W. Wang, X. H. Xiong, and Y. B. Zhang, "Extending synchronization scheme to chaotic fractional-order Chen systems," *Phys. A: Statist. Mech. Appl.*, vol. 370, no. 2, pp. 279−285, Oct. 2006.

[15] A. S. Hegazi and A. E. Matouk, "Dynamical behaviors and synchronization in the fractional order hyperchaotic Chen system," *Appl. Math. Lett.*, vol. 24, no. 11, pp. 1938−1944, Nov. 2011.

[16] M. M. Asheghan, M. T. H. Beheshti, and M. S. Tavazoei, "Robust synchronization of perturbed Chen's fractional-order chaotic systems," *Commun. Nonlinear Sci. Numer. Simul.*, vol. 16, no. 2, pp. 1044−1051, Feb. 2011.

[17] J. F. Zhao, S. Y. Wang, Y. X. Chang, and X. F. Li, "A novel image encryption scheme based on an improper fractional-order chaotic system," *Nonlinear Dyn.*, vol. 80, no. 4, pp. 1721−1729, Jun. 2015.

[18] A. S. Hegazi, E. Ahmed, and A. E. Matouk, "On chaos control and synchronization of the commensurate fractional order Liu system," *Commun. Nonlinear Sci. Numer. Simul.*, vol. 18, no. 5, pp. 1193−1202, May 2013.

[19] T. T. Hartley, C. F. Lorenzo, and H. K. Qammer, "Chaos in a fractional order Chua's system," *IEEE Trans. Circ. Syst.-I: Fund. Theory Appl.*, vol. 42, no. 8, pp. 485−490, Aug. 1995.

[20] M. Yin and L. W. Wang, "A new study in encryption based on fractional order chaotic system," *J. Electron. Sci. Technol. China*, vol. 6, no. 3, pp. 302−305, Sep. 2008.

[21] Z. Wang, X. Huang, Y. X. Li, and X. N. Song, "A new image encryption algorithm based on the fractional-order hyperchaotic Lorenz system," *Chin. Phys. B*, vol. 22, no. 1, pp. 010504, Jan. 2013.

[22] Y. Xu, H. Wang, Y. G. Li, and B. Pei, "Image encryption based on synchronization of fractional chaotic systems," *Commun. Nonlinear Sci. Numer. Simul.*, vol. 19, no. 10, pp. 3735−3744, Oct. 2014.

[23] D. L. Zhang, Y. G. Tang, and X. P. Guan, "Optimum design of fractional order PID controller for an AVR system using an improved artificial bee colony algorithm," *Acta Automat. Sin.*, vol. 40, no. 5, pp. 973−980, May 2014.

[24] D. Y. Chen, R. F. Zhang, X. Z. Liu, and X. Y. Ma, "Fractional order Lyapunov stability theorem and its applications in synchronization of complex dynamical networks," *Commun. Nonlinear Sci. Numer. Simul.*, vol. 19, no. 12, pp. 4105−4121, Dec. 2014.

[25] P. Liu and S. T. Liu, "Anti-synchronization between different chaotic complex systems," *Phys. Scr.*, vol. 83, no. 6, pp. 065006, May 2011.

[26] L. L. Huang, J. Zhang, and S. S. Shi, "Circuit simulation on control and synchronization of fractional order switching chaotic system," *Math. Comp. Simul.*, vol. 113, pp. 28−39, Jul. 2015.

[27] S. Som and S. Sen, "A non-adaptive partial encryption of grayscale images based on chaos," *Proc. Technol.*, vol. 10, pp. 663−671, Dec. 2013.

[28] X. J. Wu, Y. Li, and J. Kurths, "A new color image encryption scheme using CML and a fractional-order chaotic system," *PLoS One*, vol. 10, no. 3, pp. e0119660, Mar. 2015.

[29] M. Ahmad, U. Shamsi, and I. R. Khan, "An enhanced image encryption algorithm using fractional chaotic systems," *Proc. Comp. Sci.*, vol. 57, pp. 852−859, Dec. 2015.

[30] Y. Q. Zhang and X. Y. Wang, "A symmetric image encryption algorithm based on mixed linear-nonlinear coupled map lattice," *Inf. Sci.*, vol. 273, pp. 329−351, Jul. 2014.

[31] Y. J. Niu and X. Y. Wang, "An anonymous key agreement protocol based on chaotic maps," *Commun. Nonlinear Sci. Numer. Simul.*, vol. 16, no. 4, pp. 1986−1992, Apr. 2011.

[32] C. F. Hsu, "Intelligent control of chaotic systems via self-organizing Hermite-polynomial-based neural network," *Neurocomputing*, vol. 123, pp. 197−206, Jan. 2014.

[33] X. D. Li and S. J. Song, "Research on synchronization of chaotic delayed neural networks with stochastic perturbation using impulsive control method," *Commun. Nonlinear Sci. Numer. Simul.*, vol. 19, no. 10, pp. 3892−3900, Oct. 2014.

**Jialin Hou** graduated from Agricultural University of Shandong, China, in 1987. He received the D. E. degree from Agricultural University of China in 2005. He is currently a professor at the College of Mechanical and Electronic Engineering, Agricultural University of Shandong. His research interests include intelligent detection and automation instrument and the application of computer in agriculture.

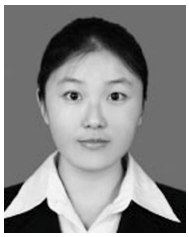

**Rui Xi** is Ph. D. candidate at the College of Mechanical and Electronic Engineering, Agricultural University of Shandong. Her research interests include automation and fractional order chaotic system.

**Ping Liu** is associate professor at the College of Mechanical and Electronic Engineering, Agricultural University of Shandong. She received her Ph. D. and M. Sc. degrees from Shandong University, in 2012 and 2007, respectively, and received her bachelor degree from Dalian University in 2006. Her research interests include control of nonlinear systems and robotics, especially the adaptive and robust control of chaos and fractal and path planning. Corresponding author of this paper.

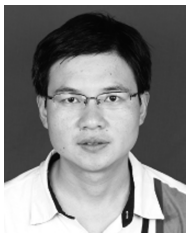

**Tianliang Liu** graduated from Technological University of Shandong, China, in 2008. He received the M. Sc. degree from Inner Mongolia University in 2011. He is currently a lecturer at Taishan Vocational and Technical College. His research interests include detection technology and automation, especially the memristor and its application.